bioRxiv preprint doi: https://doi.org/10.1101/2020.02.07.938464; this version posted February 7, 2020. The copyright holder for this preprint (which was not certified by peer review) is the author/funder, who has granted bioRxiv a license to display the preprint in perpetuity. It is made available under aCC-BY 4.0 International license.

The Nef protein of the macrophage tropic HIV-1 strain AD8 counteracts human Bst-2/tetherin

Sebastian Giese, Scott P. Lawrence, Michela Mazzon, Bernadien M. Nijmeijer, Mark Marsh#

MRC-Laboratory for Molecular Cell Biology, University College London, London, WC1E 6BT, UK

Abstract

Bst-2/tetherin inhibits the release of numerous enveloped viruses by physically attaching nascent particles to infected cells during the process of viral budding from the cell surface. Tetherin also restricts human immunodeficiency viruses (HIV), and pandemic main (M) group HIV-1s are thought to exclusively rely on their Vpu proteins to overcome tetherin-mediated restriction of virus release. However, at least one M group HIV-1 strain, the macrophage-tropic primary AD8 isolate, is unable to express *vpu* due to a mutation in its translation initiation codon. Here, using primary monocyte-derived macrophages (MDMs), we show that AD8 was able to use its Nef protein to compensate for the absence of Vpu and restore virus release to wild type levels. We demonstrate that HIV-1 AD8 Nef reduces endogenous tetherin levels from the cell surface, physically separating it from the site of viral budding and thus preventing HIV retention. Mechanistically, AD8 Nef enhances l-tetherin internalisation, leading to perinuclear accumulation of the restriction factor. Finally, we show that Nef proteins from other HIV strains also display varying degrees of tetherin antagonism. Overall, this is the first report showing that M group HIV-1s can use an accessory protein other than Vpu to antagonise human tetherin.

Bst-2 | HIV-1| Nef | tetherin | macrophages | PBMC

Correspondence: ***Mark Marsh, m.marsh@ucl.ac.uk***

Introduction

Human Immunodeficiency Virus type 1 (HIV-1) is divided into four groups, M, N, O and P, which originated from independent interspecies transmissions. The first to be discovered was Group M representing the principal global pandemic form of HIV-1. The success of group M has been attributed to its ability to mount a potent anti-tetherin defence in humans [1,2]. Bst-2/tetherin is a 20 kDa glycoprotein that restricts the release of a broad range of enveloped viruses from infected host cells [3]. Tetherin has two membrane-association domains: The N-terminus is a type-2 transmembrane domain, while the C-terminus is linked to glycophosphatidylinositol (GPI). During viral budding, the tetherin N-terminal transmembrane domain remains embedded in the host cell membrane but the C-terminal domain can be incorporated into the viral membrane, thus tethering nascent virions and preventing virus release [4]. Physically tethered virions can then be internalised and degraded, limiting spread of the virus. Tetherin potently restricts human HIV [5,6], and overcoming this restriction was suggested to have been a prerequisite for the pandemic spread of HIV-1 [2].

Main (M) group HIV-1s are thought to exclusively rely on their Vpu proteins to antagonise human tetherin and ensure efficient virus release from infected cells [7]. Interaction between the tetherin and Vpu transmembrane domains enables the C-terminus of Vpu to displace tetherin from the site of viral budding and enhances sorting of tetherin to lysosomes and its degradation [8-12]. However, other HIV proteins have the ability to antagonise tetherin: For example, HIV-2 lacks a Vpu protein but has adapted its envelope (Env) protein to enhance tetherin internalisation, thereby removing the restriction factor from its site of action [13]. Additionally, outlier (O) group HIV-1s and many simian immunodeficiency viruses (SIV) use their Nef proteins to antagonise the tetherin proteins of their respective hosts [14,15].

Nef is a 23 kDa HIV/SIV accessory protein that associates with the cytoplasmic leaflet of the plasma membrane via an N-terminal myristic acid moiety. The Nef protein of macaque-infecting SIV (SIVmac) recruits AP-2 complexes to macaque tetherin, which enhances clathrin-mediated endocytosis of tetherin and reduction of cell surface tetherin levels, though this does not lead to tetherin degradation [16]. Due to a five-residue deletion in the N-terminal cytoplasmic tail of human tetherin, SIV Nef proteins are unable to antagonise human tetherin using this mechanism [2,16,17] and this could be a reason for these viruses to adapt Vpu for tetherin antagonism [1]. However, to date no HIV-1 M group Nef has been described to counteract human tetherin.

In light of these findings, the identification of AD8, a group M primary isolate that was able to efficiently replicate in monocyte-derived macrophages (MDMs) and PBMCs in the absence of Vpu was puzzling [18]. Here we show that the AD8 Nef protein counteracts human tetherin by decreasing the concentration of endogenous tetherin at the surface of primary human macrophages, which in turn reduces virus retention. Mechanistically, AD8 Nef promotes tetherin internalisation and perinuclear accumulation without causing tetherin degradation. Both N- and C-terminal domains of AD8 Nef contribute to reducing tetherin levels at the cell surface, which is observed for l-, but not s-tetherin. This is the first study showing that

bioRxiv preprint doi: https://doi.org/10.1101/2020.02.07.938464; this version posted February 7, 2020. The copyright holder for this preprint (which was not certified by peer review) is the author/funder, who has granted bioRxiv a license to display the preprint in perpetuity. It is made available under aCC-BY 4.0 International license.

some strains of M group HIV-1s encode a tetherin antagonist other than Vpu.

Material and Methods

Reagents and antibodies

Tissue culture media and supplements were purchased from Life Technologies (Paisley, UK), fetal calf serum (FCS) from PAA (Little Chalfont, UK), human AB serum from PAA and Sigma-Aldrich (Dorset, UK), and tissue culture plastic from Thermo Fisher Scientific (Waltham, USA) and TPP (Trasadingen, Switzerland). DNA-modifying enzymes were from Promega (Southampton, UK) and chemicals from Sigma-Aldrich, unless specified otherwise.

Antibodies to HIV-1 p24/p55 Gag (38:96K and EF7), HIV-1 Env (b12 and 2G12) and HIV-1 Nef (2/81c/2j), as well as antiserum to HIV-1 p24/p55 Gag (ARP432), were obtained from the NIBSC Centre for AIDS Reagents (South Mimms, UK), and rabbit antiserum to Bst-2/tetherin (cat. no. 11721) from the NIH AIDS Reagent Program (Germantown, USA). Sheep antiserum to HIV-1 Nef was provided by M. Harris (University of Leeds, UK), rabbit antiserum to Vpu (U2-2) by K. Strebel (NIAID, Bethesda, USA), and anti-VSVG (P5D4) by T. Kreis (UNIGE, Geneva, Switzerland). Anti-adaptin γ (clone 88) was purchased from BD Biosciences (Oxford, UK), polyclonal anti-Bst-2/tetherin (B02P) from Abnova (Taipei, Taiwan), anti-CD81 (M38) from Abcam (Cambridge, UK), anti-HRP from Jackson ImmunoResearch (West Grove, USA), anti-p65 from Santa Cruz Biotechnology (Heidelberg, Germany), anti-TGN46 (AHP500G) from AbD Serotec (Kidlington, UK), Alexa Fluor-conjugated antibodies from Life Technologies, highly cross-adsorbed DyLight 405-conjugated goat anti-mouse, as well as HRP-conjugated antibodies, from Thermo Fisher Scientific, and IRDye secondary reagents from Li-COR Biosciences (Cambridge, UK).

DNA plasmids

The origins and descriptions of all DNA plasmids used in this study are listed in Table S1.

Proviral plasmids and virus stocks

The HIV-1 molecular clones AD8(+), AD8(-) and AD8(U_{del2}) were provided by K. Strebel (NIAID, Bethesda, USA) (21). To obtain AD8(+)ΔNef, AD8(-)ΔNef and AD8(U_{del2})ΔNef, the third methionine codon in Nef was disrupted by introducing an adenine at nucleotide position 60, which causes a frameshift and a premature stop codon ten nucleotides downstream (see supplementary information for details).

HIV-1 AD8 stocks were prepared as described previously [35]. Stocks of VSVG-pseudotyped HIV-1 AD8 were prepared by co-transfecting HEK 293T cells with proviral and VSVG DNA for two days and then clearing the culture supernatants of cell debris by centrifugation.

p24 ELISA assay

Gag p24 levels in cell-free supernatants from HIV-1-infected cells were quantified using the HIV-1 p24CA Antigen Capture Assay Kit (AIDS and Cancer Virus Program, National Cancer Institute, Frederick, USA) according to the manufacturers' instructions.

Single-cycle infectivity assay

Single-cycle infectivities of HIV-1 AD8 stocks were determined as described previously [35]. Single-cycle infectivities of VSVG-pseudotyped HIV-1 AD8 were determined by infecting HeLa cells with serial dilutions of virus stocks for two days and quantifying the proportion of infected cells by flow cytometry, as described below.

Cells, transfections and infections

HeLa, HEK 293, HEK 293T, and HeLa TZM-bl cells were maintained in DMEM with GlutaMAX supplemented with 10% FCS, 100 U/ml penicillin and 0.1 mg/ml streptomycin. HEK 293 cells stably expressing s- or l-tetherin were provided by S. Neil (KCL, London, UK, [23]) and maintained in the presence of 100 µg/ml hygromycin B (Life Technologies).

Where indicated, HeLa and HEK cells were transfected for two days with TransIT-HeLaMONSTER (Cambridge BioScience, Cambridge, UK) or FuGENE HD (Promega), respectively, according the manufacturers' instructions. HIV-1 AD8 Env was co-transfected with HIV-1 Rev at a ratio of 3:1. For tetherin titrations, HEK 293T cells were seeded in 12-well plates and co-transfected with 400 ng proviral AD8 DNA and 400 ng tetherin-encoding DNA, or vector DNA, using FuGENE6 (Promega) according to the manufacturer's instructions.

To infect HeLa cells with VSVG-pseudotyped HIV-1 AD8, cells were incubated with 0.3-0.4 IU/cell overnight, followed by a media change and another 24 h incubation before harvest.

MDMs were prepared from peripheral blood mononuclear cells (PBMC) isolated from buffy coats from healthy blood donors (National Blood Service, Essex, UK), as described previously [36], and differentiated in complete monocyte derived macrophage (MDM) medium containing 10 ng/ml M-CSF (R&D Systems, Abingdon, UK) for two days. Seven-day-old MDMs were infected with HIV-1 AD8 (3 IU/cell) by spinoculation for 2 h at 1,300 g and cultured for a further seven days. Unless specified otherwise, MDMs were used after 14 days in culture.

Western blot analysis

Cells were washed in PBS and lysed in non-reducing Laemmli buffer (4% SDS, 20% glycerol, 0.125 M Tris-HCl pH 6.8, bromophenol blue) for 10 min at 95°C. Virus lysates were prepared by pelleting virus-containing culture supernatants through 20% sucrose cushions for 1.5-2 h at 100,000 *g* and 4°C. Pellets were

bioRxiv preprint doi: https://doi.org/10.1101/2020.02.07.938464; this version posted February 7, 2020. The copyright holder for this preprint (which was not certified by peer review) is the author/funder, who has granted bioRxiv a license to display the preprint in perpetuity. It is made available under aCC-BY 4.0 International license.

resuspended in Laemmli sample buffer and heated to 95°C for 10 min.

Western blot analysis was performed essentially as described previously [35]. Lysates were separated on SDS-polyacrylamide gels and transferred either to Immobilon-P or Immobilon-FL PVDF membranes (Millipore, Watford, UK) under semi-dry blotting conditions. Blots were quenched, incubated with primary antibody at 4°C overnight, washed and incubated with either the appropriate HRP-conjugated secondary antibody or IRDye secondary antibody for 1 h at room temperature. After five washes, membranes were either briefly incubated in SuperSignal West Pico/Dura/Femto Chemiluminescent Substrate (Thermo Fisher Scientific) and signals detected with Amersham Hyperfilm ECL (GE Healthcare Life Sciences, Little Chalfont, UK), or directly imaged on an Odyssey infrared imaging system (LiCOR).

All tetherin blots were performed under non-reducing conditions using the polyclonal Bst-2 antibody B02P. For all other blots, 100 mM dithiothreitol was added to the lysates before gel electrophoresis.

Flow cytometry analysis

For flow cytometry analysis of cell surface tetherin or HIV-1 Env levels, cells were incubated for 1 h on ice in DMEM with GlutaMAX/FCS/penicillin/streptomycin or complete MDM medium containing rabbit antiserum to Bst-2, 10 µg/ml polyclonal Bst-2 antibody (B02P), or 10 µg/ml monoclonal anti-Env (b12) antibody. For HEK cells, 15 µg/ml anti-CD81 (M38) antibody was added during cell surface staining. Cells were washed once with ice-cold PBS, fixed in 4% PFA (TAAB, Reading, UK), scraped off the tissue culture dish, permeabilised with 0.1% saponin/1% FCS/2 mM EDTA/0.05% sodium azide/PBS, immunolabelled for 1 h with additional primary antibody, washed three times in 0.1% saponin/1% FCS/2 mM EDTA/0.05% sodium azide/PBS, incubated for 30 min with appropriate Alexa Fluor-conjugated secondary antibodies, washed three times and analysed on an LSR II flow cytometer (BD Biosciences). For flow cytometry of MDMs, FCS was replaced by human AB serum, and 6 µg/ml human IgG was added during permeabilisation. For single-cycle infectivity assays of VSVG-pseudotyped HIV-1 AD8, infected HeLa cells were fixed, scraped off the tissue culture dish and processed for flow cytometry, as described above. Data were analysed using FlowJo software (TreeStar, Ashland, USA). Transfected cells were identified by immunostaining for the transfected proteins, or by GFP expression. Infected cells were identified by immunostaining for p24/p55 Gag. Relative cell surface tetherin/Env levels were calculated by dividing the median fluorescent intensities (MFI) of the transfected/infected cells by the MFI of the untransfected/uninfected cells of the same populations, unless specified otherwise.

Intracellular tetherin immunofluorescence

For intracellular tetherin immunofluorescence, transfected tetherin-expressing HEK cells were washed with PBS, fixed in 4% formaldehyde, quenched with 50 mM NH_4Cl and permeabilised with 0.1% Triton X-100/0.5% BSA/PBS. Cells were labelled for 1.5 h with 10 µg/ml mouse anti-Bst-2 (B02P), 1:100 rat anti-Nef serum, 2.5 µg/ml sheep anti-TGN46 and 1 µg/ml rabbit anti-p65 diluted in 0.5% BSA/PBS, washed in 0.5% BSA/PBS and incubated for 1 h with fluorescent secondary antibodies. Samples were washed and coverslips mounted in Mowiol. Confocal images were acquired with an inverted Leica TCS SP3 confocal microscope, 63x oil objective (NA 1.4) and LAS AF software, and processed using Fiji. An ImageJ macro was written for semi-automated analysis of perinuclear tetherin accumulation. Briefly, the macro segmented the area occupied by all cells (using p65 as a cytosolic marker), Nef-expressing cells (using Nef as a marker) and the area occupied by TGN (using TGN46 as a marker). It then superimposed selections of the cell/transfected cell and TGN areas onto the respective tetherin stainings and measured the tetherin mean fluorescent intensities for both selections. To calculate TGN enrichment of tetherin, the TGN tetherin signal was divided by the tetherin signal from the residual cell and normalised to mock transfected samples.

Cell surface tetherin immunofluorescence

For cell surface tetherin immunofluorescence, MDMs were incubated for 1 h on ice in complete MDM medium containing 10 µg/ml anti-Bst-2 (B02P). Cells were washed with ice-cold PBS, fixed in 4% PFA, quenched with 50 mM NH_4Cl and permeabilised with 0.1% Triton X-100/0.5% BSA/6 $\mu g.ml^{-1}$ human IgG in PBS. Cells were labelled for 1.5 h with primary antibodies diluted in 0.5% BSA/6 $\mu g.ml^{-1}$ human IgG/PBS, washed in 0.5% BSA/PBS and incubated for 1 h with appropriate combinations of fluorescent secondary antibodies. Samples were washed, DNA stained with 10 µg/ml Hoechst 33258 in PBS, and coverslips mounted in Mowiol. Confocal images were acquired with an inverted Leica TCS SP5 confocal microscope, 63x oil objective (NA 1.4) and LAS AF software, and processed using Fiji.

Statistical analysis

Standard errors of the mean (SEM) and p values are based on all replicates of at least three independent experiments. P values were calculated using the unpaired Student's t-test, unless indicated otherwise.

Results

HIV-1 AD8 Nef reduces cell surface tetherin levels

Although evidence suggests that efficient counteraction of tetherin is required for HIV spread [2], the ADA-derived M group HIV-1 molecular clone AD8 effectively replicates in macrophages in the absence of

bioRxiv preprint doi: https://doi.org/10.1101/2020.02.07.938464; this version posted February 7, 2020. The copyright holder for this preprint (which was not certified by peer review) is the author/funder, who has granted bioRxiv a license to display the preprint in perpetuity. It is made available under aCC-BY 4.0 International license.

Vpu [19]. Consistently, monocyte-derived macrophages (MDM) infected with AD8 containing the start codon mutation in Vpu [AD8 (-)] or with a clone of AD8 where Vpu has been reconstituted [AD8 (+)], release similar levels of virus [Figure 1A and [18]]. These observations suggest that AD8 may have evolved a mechanism to antagonise human tetherin independent from Vpu. Indeed, in AD8-infected MDMs we observed significantly lower levels of surface tetherin than in uninfected cells (Figure 1B and 1C).

To identify additional tetherin antagonists in AD8, we transfected candidate AD8 proteins, AD8 Env or Nef, or start codon repaired AD8 Vpu into HeLa cells, that express endogenous human tetherin. After two days the cell surface tetherin levels were quantified by flow cytometric analysis. We found that AD8 start codon repaired Vpu reduced cell surface tetherin by around 85%, whereas AD8 Env had no effect (Figure 2A). Surprisingly, AD8 Nef also reduced cell surface tetherin by around 60% (Figure 2A).

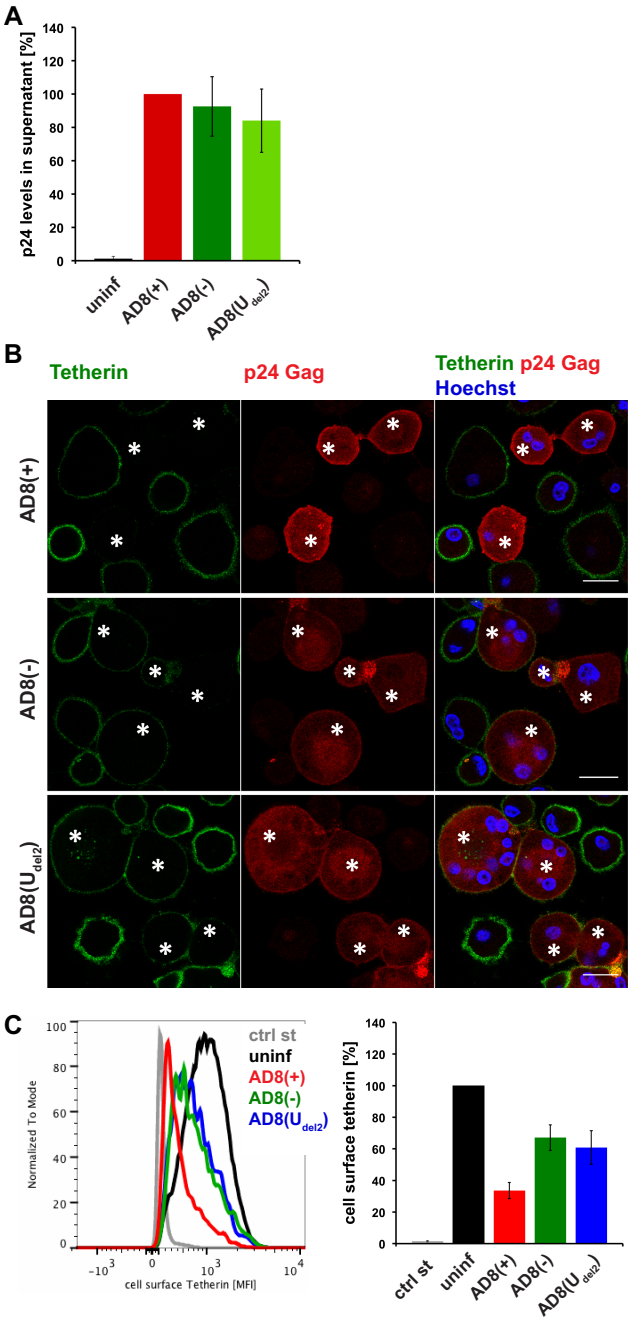

Figure 1: HIV-1 AD8-infected macrophages show low levels of cell surface tetherin and high levels of virus release in the absence of Vpu. (A) p24 Gag concentrations in cell-free culture supernatants from AD8-infected MDMs were determined using ELISA. (B) AD8-infected MDMs were stained for cell surface tetherin and intracellular p24 Gag. Asterisks mark infected cells. Single confocal sections are shown. Scale bars = 20 µm. (C) Cell surface tetherin levels of AD8-infected MDMs were analysed by flow cytometry. Uninfected MDMs were immunolabelled with anti-VSVG as a staining control. The left-hand panel shows the result from a representative experiment, the right-hand panel the average relative tetherin mean fluorescence intensities of three donors ± standard error of the mean (SEM). Bars represent the relative means ± SEM of triplicate samples from three donors.

bioRxiv preprint doi: https://doi.org/10.1101/2020.02.07.938464; this version posted February 7, 2020. The copyright holder for this preprint (which was not certified by peer review) is the author/funder, who has granted bioRxiv a license to display the preprint in perpetuity. It is made available under aCC-BY 4.0 International license.

To establish whether AD8 Nef also counteracts tetherin at expression levels reached during infection, we used HIV-1 AD8 proviruses used in previous studies [18,20]. Since mutations in the Vpu start codon can enhance Env expression, we also used AD8(U_{del2}), which carries an internal deletion in Vpu that abolishes Vpu expression [18,20]. For each of these Vpu mutants we generated a Nef-negative variant AD8 ΔNef, which carries a premature stop codon in Nef (Table. S1). When we infected HeLa cells with VSVG-pseudotyped HIV-1 AD8 for two days, the Vpu-negative Nef-expressing AD8(-) and AD8(U_{del2}) still reduced cell surface tetherin by around 55% (Figure 2B), confirming that AD8 Nef antagonises tetherin at physiological concentrations. The Vpu-positive AD8(+) and AD8(+)ΔNef reduced cell surface tetherin by around 85%, whereas the Nef- and Vpu-negative AD8(-)ΔNef and AD8(U_{del2}) had no effect (Figure 2B).

Cell surface tetherin retains nascent virions at the surface of virus producing cells. To test whether AD8 Nef-mediated tetherin antagonism reduces virus tethered to the cell surface, we infected HeLa cells with VSVG-pseudotyped HIV-1 AD8 and quantified cell surface Env by flow cytometry. As expected, the Vpu negative Nef positive AD8(-) and AD8(U_{del2}) showed 1.7-fold less α-Env reactivity than the Vpu and Nef negative AD8(-)ΔNef and AD8(U_{del2})ΔNef, respectively (Figure 2C). Thus, AD8 Nef-mediated tetherin antagonism functionally reduces virus tethering to the cell surface.

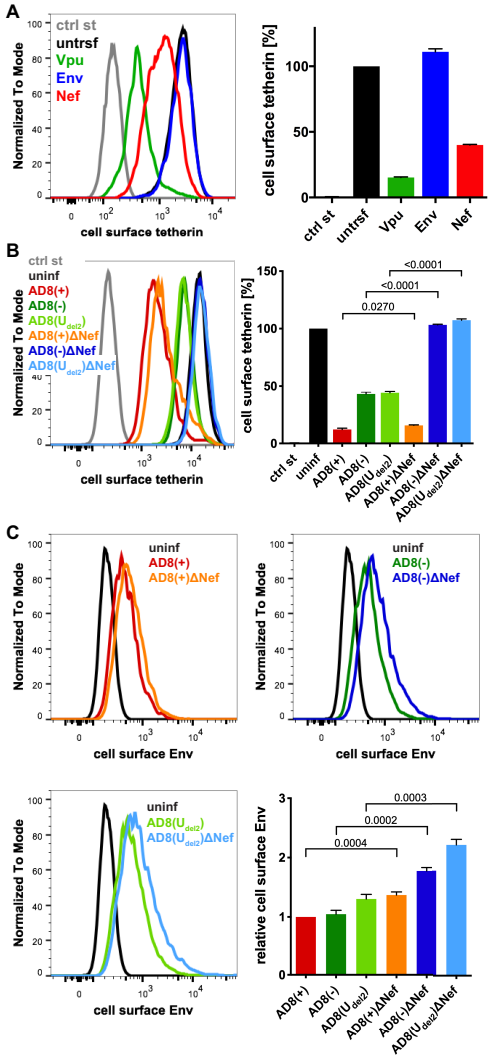

Figure 2: HIV-1 AD8 Nef reduces cell surface tetherin levels and tethered virions. (A) AD8 Vpu, Env, or Nef were transfected into HeLa cells for two days. Cell surface tetherin levels were quantified by immunolabelling the restriction factor on ice prior to formaldehyde fixation, cell permeabilization, immunolabelling for Vpu, Env, or Nef, labelling with fluorescent secondary antibodies and flow cytometry. Mock-transfected cells were immunolabelled with anti-VSVG as a staining control. The left-hand panel shows the result from a representative experiment, the right-hand panel shows the average relative tetherin levels from three independent experiments ± standard error of the mean (SEM). (B) Cell surface tetherin levels of VSVG-pseudotyped AD8-infected or uninfected HeLa cells were quantified by flow cytometry. Uninfected cells were immunolabelled with anti-HRP as a staining control. The left-hand panel shows the result from a representative experiment, the right-hand panel the average relative tetherin levels from four independent experiments ± SEM with relevant P values. (C) Cell surface Env levels of VSVG-pseudotyped AD8-infected or uninfected HeLa cells were quantified by flow cytometry. The upper panels and lower left-hand panel show the results from a representative experiment, the lower right-hand panel shows the average relative Env levels from four independent experiments ± SEM with relevant P values.

bioRxiv preprint doi: https://doi.org/10.1101/2020.02.07.938464; this version posted February 7, 2020. The copyright holder for this preprint (which was not certified by peer review) is the author/funder, who has granted bioRxiv a license to display the preprint in perpetuity. It is made available under aCC-BY 4.0 International license.

HIV-1 AD8 Nef reduces cell surface tetherin levels and enhances virus release in primary macrophages

To confirm that AD8 Nef antagonises human tetherin in macrophages, we infected primary MDMs with the panel of viruses described above for seven days, and quantified cell surface tetherin levels by flow cytometry. Similar to our observations in HeLa cells (Figure 2B), MDMs infected with the Nef-expressing AD8(-) and AD8(U_{del2}) showed almost two-fold lower cell surface tetherin levels than cells infected with the Nef-negative AD8(-)ΔNef and AD8(U_{del2})ΔNef (Figure 3A). Thus, AD8 Nef also depletes cell surface tetherin in primary macrophages.

We next tested whether AD8 Nef-mediated counteraction of tetherin enhances virus release from MDMs. While the highest levels of virus release were observed for cells infected with the Vpu-positive AD8(+) and AD8(+)ΔNef (Figure 3B), AD8(-) and AD8(U_{del2}) infected cells released more virus than AD8(-)ΔNef and AD8(U_{del2})ΔNef-infected MDMs, respectively (Figure 3B) indicating that Nef compensates for the loss of Vpu-mediated tetherin antagonism. Interestingly, western blot analyses of the MDM lysates revealed that significantly less p24 Gag was associated with AD8(-) and AD8(U_{del2}) infected cells than with AD8(-)ΔNef and AD8(U_{del2})ΔNef infected cells (Figure 3B). Since p24 Gag is only found in mature HIV, and cell-associated p24 Gag serves as a marker for retained virus, these observations show that more HIV is retained in the absence of AD8 Nef than in its presence. Overall, these findings demonstrate that on primary macrophages AD8 Nef reduces cell surface tetherin, virus retention and promotes virus release.

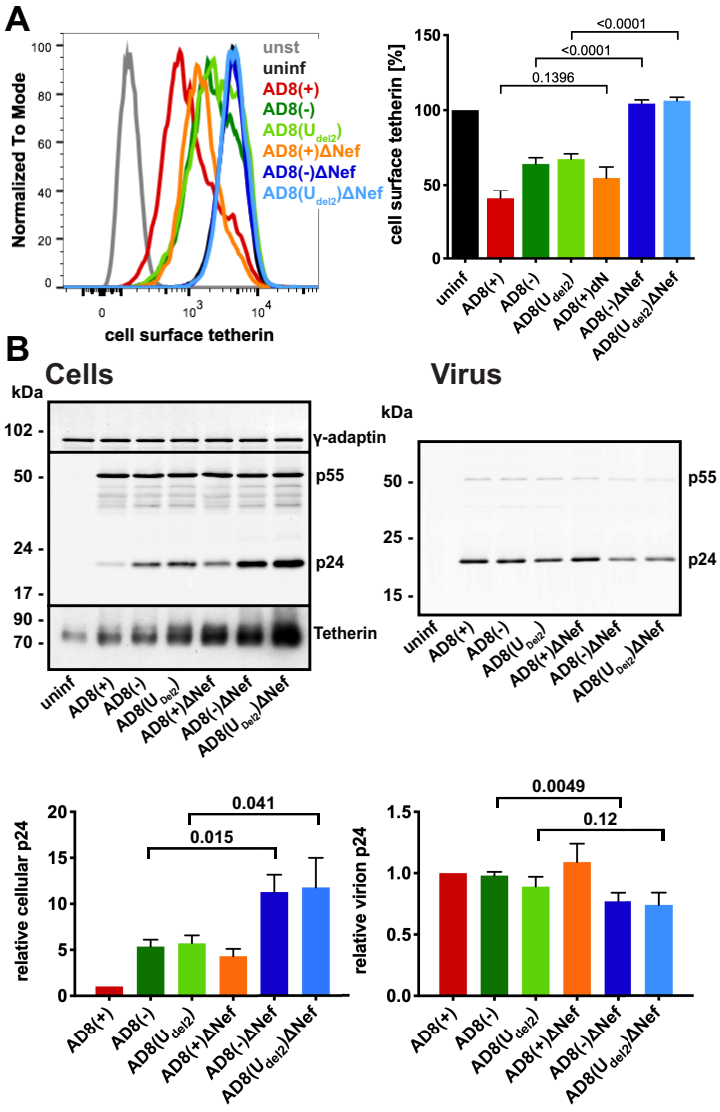

Figure 3: HIV-1 AD8 Nef antagonises tetherin in primary macrophages. (A) MDMs were infected with AD8 for seven days and cell surface tetherin levels quantified by flow cytometry. Uninfected cells were immunolabelled with anti-HRP as a staining control. The left-hand panel shows the result from a representative experiment, the right-hand panel the average relative tetherin levels from five donors ± SEM with relevant P values. (B) MDMs were infected with HIV-1 AD8 for seven days. Virus and the corresponding cells were lysed and analysed by western blotting. The top panel shows representative western blots. The graphs in the bottom panel show the average relative cell and virus p24 Gag levels from four donors ± SEM with relevant P values.

bioRxiv preprint doi: https://doi.org/10.1101/2020.02.07.938464; this version posted February 7, 2020. The copyright holder for this preprint (which was not certified by peer review) is the author/funder, who has granted bioRxiv a license to display the preprint in perpetuity. It is made available under aCC-BY 4.0 International license.

HIV-1 AD8 Nef reduces cell surface l-tetherin levels and increases virus release

In addition to the full length tetherin molecule (denoted long- or l-tetherin), a short isoform (s-tetherin) that lacks 12 N-terminal amino acid residues is generated by alternative translation initiation from a downstream start codon [21]. Both s- and l-tetherin physically retain nascent virions, but virus-associated l-tetherin can also trigger pro-inflammatory NFκB signalling that enhances viral restriction [21,22]. To examine whether AD8 Nef counteracts s- and l-tetherin, we transfected AD8 Nef into HEK cells stably expressing either s- or l-tetherin [23] and quantified cell surface tetherin by flow cytometry. AD8 Nef reduced the cell surface levels of l-tetherin by around 45%, but only caused a 10% drop in the cell surface levels of s-tetherin (Figure 4A). Thus, AD8 Nef primarily reduces the amount of of l-tetherin expressed at the cell surface.

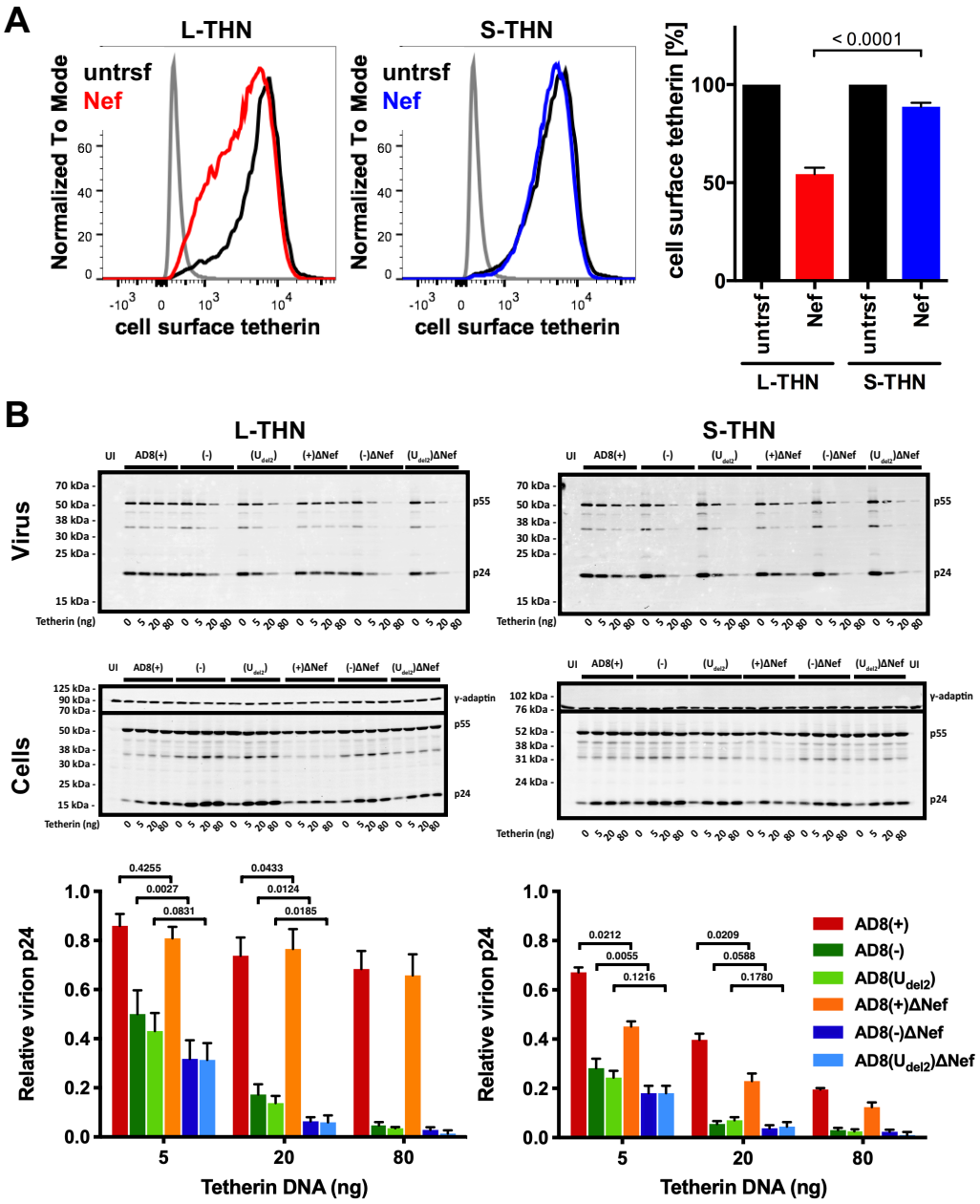

Figure 4: HIV-1 AD8 Nef antagonises the long isoform of tetherin and moderately increases virus release. (A) HEK 293 cells expressing s- or l-tetherin were transfected with AD8 Nef or a control plasmid for two days, and cell surface tetherin levels were quantified by flow cytometry. Mock-transfected cells were immunolabelled with anti-HRP as a staining control. To discriminate intact cells from debris, all cells were also stained and gated for cell surface CD81. The left-hand and central panels show the result from a representative experiment, the right-hand panel the average relative tetherin levels from three independent experiments ± SEM with relevant P values. (B) HEK 293T cells were transfected with 400 ng of HIV-1 AD8 proviral DNA and increasing amounts of l- or s-tetherin-encoding plasmids. Virus and corresponding cells were harvested two days post transfection, and all lysates were analysed by western blotting. Virus p24 Gag levels were normalised to cellular p55 Gag. The graphs show the average relative virus p24 Gag levels from at least four independent experiments ± SEM with relevant P values. Tetherin expression was confirmed as shown in Figure S1A.

bioRxiv preprint doi: https://doi.org/10.1101/2020.02.07.938464; this version posted February 7, 2020. The copyright holder for this preprint (which was not certified by peer review) is the author/funder, who has granted bioRxiv a license to display the preprint in perpetuity. It is made available under aCC-BY 4.0 International license.

We next investigated whether the AD8 Nef-mediated decrease in cell surface levels of l-tetherin promotes virus release. We co-transfected proviral HIV-1 AD8 together with increasing amounts of s- or l-tetherin DNA into HEK cells for two days, then harvested the cells and cell supernatants and quantified virus release by ultracentrifugation and western blot analysis of culture supernatants (Figure 4B, S1A). At low concentrations of l-tetherin (20 ng transfected plasmid DNA), release of the Nef-positive AD8(-) and AD8(U_{del2}) viruses was significantly higher than that of the Nef-negative AD8(-)ΔNef and AD8(U_{del2})ΔNef (Figure 4B). The highest levels of virus release were observed for the Vpu-positive AD8(+) and AD8(+)ΔNef (Figure 4B). Thus, HIV-1 AD8 Nef reduces the cell surface levels of l-tetherin and thereby enhances virus release.

N- and C-terminal domains of HIV-1 AD8 Nef contribute to the reduction in cell surface tetherin

The Nef proteins of many HIV-1 strains, including NL4.3, are thought to be inactive toward human tetherin. Indeed, NL4.3 Nef did not significantly decrease cell surface tetherin levels when we transfected HeLa cells and quantified tetherin by flow cytometry (Figure 5). To determine which AD8 Nef domains mediate tetherin antagonism, we generated chimeric Nef proteins that comprise the N-terminal 85 residues of AD8 Nef and the C-terminal 122 residues of NL4.3 (AD8-NL4.3 Nef), or the N-terminal domain of NL4.3 and the C-terminal domain of AD8 Nef (NL4.3-AD8 Nef). When transfected into HeLa cells, both AD8-NL4.3 and NL4.3-AD8 Nef reduced cell surface tetherin levels by 45% and 30%, respectively, whereas AD8 Nef caused a 55% drop in cell surface tetherin (Figure 5). In addition, mutating the N-terminal myristoylation signal, previously shown to prevent Nef association with membranes [24], significantly impaired AD8 Nef's ability to reduce cell surface tetherin levels (G2A; Figure S2A). Thus, membrane-association is essential for, and both the N- and C-terminal domains contribute to, AD8 Nef-mediated antagonism of human tetherin.

HIV-1 AD8 Nef enhances tetherin internalisation and causes perinuclear tetherin accumulation

When we infected MDMs with HIV-1 AD8 and analysed the cell lysates by western blotting, we did not find consistent differences between the total cell tetherin levels in AD8(-)/ AD8(U_{del2}) and AD8(-)ΔNef/ (U_{del2})ΔNef infected cells (Figure 3B, and Figure S3), suggesting that AD8 Nef does not promote tetherin degradation. To further investigate the mechanism by which AD8 Nef reduces cell surface tetherin, we transfected AD8 Nef into tetherin-expressing HEK cells. Confocal imaging revealed that AD8 Nef-expression caused a perinuclear accumulation of l-tetherin that partially overlapped with the *trans*-Golgi network marker TGN46 (Figure 6A). No such intracellular accumulation was observed in AD8-Nef-transfected s-tetherin-expressing cells, or in mock-transfected cells (Figure 6A). ImageJ-based quantification confirmed that AD8 Nef expression caused significantly more perinuclear accumulation of l- than of s-tetherin (Figure 6A).

Intracellular tetherin accumulation may be caused either by impaired anterograde trafficking from the TGN to the cell surface or enhanced internalisation from the cell surface, or both. Since SIVmac Nef enhances macaque tetherin internalisation without causing its degradation [23], we hypothesised that HIV-1 AD8 Nef might employ a similar mechanism with human tetherin. To test this hypothesis, we transfected HeLa cells with AD8 Nef for two days, immunolabelled cell surface tetherin on ice, then warmed the cells to 37°C to allow internalisation, and quantified residual cell surface tetherin by flow cytometry. As expected, when tetherin was not internalised (0 min), cell surface tetherin levels were about 55% lower on AD8 Nef-positive cells than on Nef-negative cells in the same population (Figure 6B and Figure S2B). However, when all graphs were normalised to this first time point (0 min), we observed almost linear tetherin internalisation for the first 30 min after warm-up (Figure S2B). Linear regression analysis revealed that the rate of tetherin internalisation was almost 1.5 times higher in AD8 Nef-positive than in Nef-negative cells (Figure 6B). Consistently, mutating one or both of the two AP-2 binding motifs in AD8 Nef slightly, but significantly, reduced Nef-mediated cell surface tetherin reduction (Figure S2A). Thus, AD8 Nef removes tetherin from the cell surface by enhancing its internalisation, which in part at least contributes to perinuclear accumulation of the restriction factor.

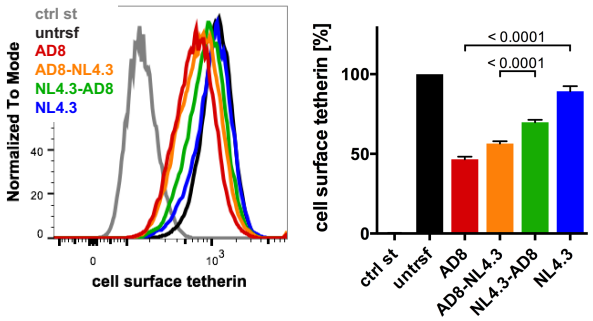

Figure 5: N- and C-terminal domains of HIV-1 AD8 Nef contribute to its anti-tetherin activity. HeLa cells were transfected with AD8 Nef, HIV-1 NL4.3 Nef, or chimeric Nef proteins that contain the N-terminal 85 residues of AD8 Nef and the C-terminal 122 residues of NL4.3 Nef (AD8-NL4.3 Nef) or vice versa (NL4.3-AD8 Nef). Two days post transfection cell surface tetherin levels were quantified by flow cytometry. Mock-transfected cells were immunolabelled with anti-HRP as a staining control. The left-hand panel shows the results of a representative experiment, the right-hand panel the average relative tetherin levels from four independent experiments ± SEM with relevant P values.

bioRxiv preprint doi: https://doi.org/10.1101/2020.02.07.938464; this version posted February 7, 2020. The copyright holder for this preprint (which was not certified by peer review) is the author/funder, who has granted bioRxiv a license to display the preprint in perpetuity. It is made available under aCC-BY 4.0 International license.

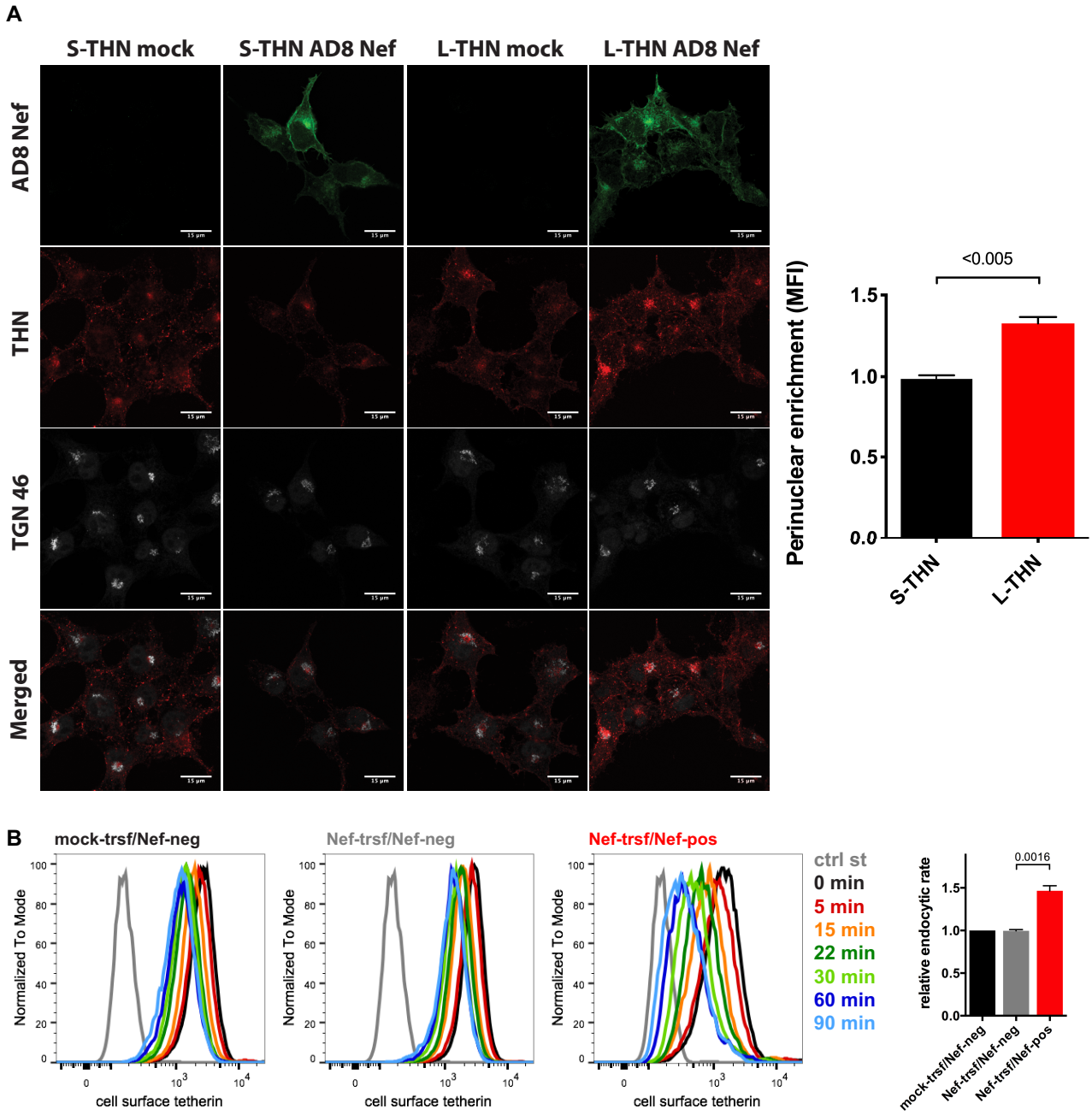

Figure 6: HIV-1 AD8 Nef antagonises tetherin by enhanced internalisation and perinuclear accumulation. (A) HEK cells expressing s- or l-tetherin were transfected with AD8 Nef or a control plasmid for two days then fixed and stained for intracellular tetherin. Single confocal sections from a representative experiment are shown. Scale bars = 15 µm. The graph shows accumulation of tetherin in a TGN46-positive perinuclear region in AD8 Nef-expressing cells. All values are normalised to mock-transfected cells, so that a value of 1 indicates no tetherin enrichment. The data show the average of three independent experiments ± SEM with relevant P values. (B) AD8 Nef- or mock-transfected HeLa cells were immunolabelled for tetherin on ice and shifted to 37°C for various times. Residual cell surface tetherin antibody was then revealed by immunostaining on ice with a fluorescent secondary antibody. Cells were fixed, permeabilised, immunostained for Nef and analysed by flow cytometry. The three left-hand panels show the result from a representative experiment for mock-transfected cells, or AD8 Nef-transfected cells that did (Nef-pos) or did not (Nef-neg) express Nef. The right-hand panel shows the average endocytic rates from four independent experiments ± SEM during the first 30 min at 37°C with relevant P values. Endocytic rates were derived from the regression analysis shown in Figure S2B.

bioRxiv preprint doi: https://doi.org/10.1101/2020.02.07.938464; this version posted February 7, 2020. The copyright holder for this preprint (which was not certified by peer review) is the author/funder, who has granted bioRxiv a license to display the preprint in perpetuity. It is made available under aCC-BY 4.0 International license.

Nef proteins from different HIV strains reduce cell surface tetherin to various degrees

Finally, we examined whether the Nef proteins from other HIV strains also reduce the cell surface levels of human tetherin. We transfected IRES GFP constructs encoding Nef proteins from a range of HIV strains into HeLa cells and quantified cell surface tetherin levels two days later by flow cytometry. Consistent with our previous results, AD8 Nef reduced tetherin levels by around 55% (Figure 7). HIV O-group Nef proteins (OMRCA and 13127K2), which have been described to antagonise human tetherin [14], reduced cell surface tetherin levels by around 70% (Figure 7). Interestingly, Nef proteins from HIV-1 M group strains SF2, CH077 and CH198, as well as from the HIV-1 P group strain RBF168, reduced tetherin levels to a similar extent as AD8 Nef. By comparison, Nef proteins from the HIV-1 M group strains NL4.3, JR-CSF, the HIV-1 N group strain 2693BA and the HIV-2 strain 7312, showed smaller effects (Figure 7). An IRES GFP control construct that does not encode a functional Nef protein did not reduce cell surface tetherin levels (Figure 7). While this overexpression system can only provide an indicative measure of tetherin reduction across strains, this dataset suggests that Nef proteins from various HIV-1 strains possess some degree of anti-tetherin activity.

Discussion

Globally, M group HIV-1 infections account for more than 99% of HIV infections. The ability of these viruses to overcome the cellular restriction imposed by tetherin has been viewed as a key step in the global spread of HIV [2], thus understanding how M group HIV-1s counteract tetherin is important. Although it is known that HIV-1 Vpu is an efficient antagonist of human tetherin, we report here for the first-time that at least one M group HIV-1, the macrophage tropic AD8, uses its' Nef protein to antagonise this key restriction factor.

When the HIV-1 molecular clone AD8 was derived from the primary isolate ADA, it encoded an inactivating start codon mutation in Vpu [19]. As AD8 can sustain high levels of virus release from infected cells in the absence of Vpu, initial reports concluded that the viral Env protein possesses Vpu-like activity [18]. However, while a later study confirmed that high levels of Vpu-deficient AD8 are released, they failed to find evidence for Env involvement [25]. Consistent with this latter study, we show that AD8 Env does not reduce cell surface tetherin expression on HeLa cells (Figure 2A). Instead, we found that AD8 Nef decreases cell surface tetherin levels by

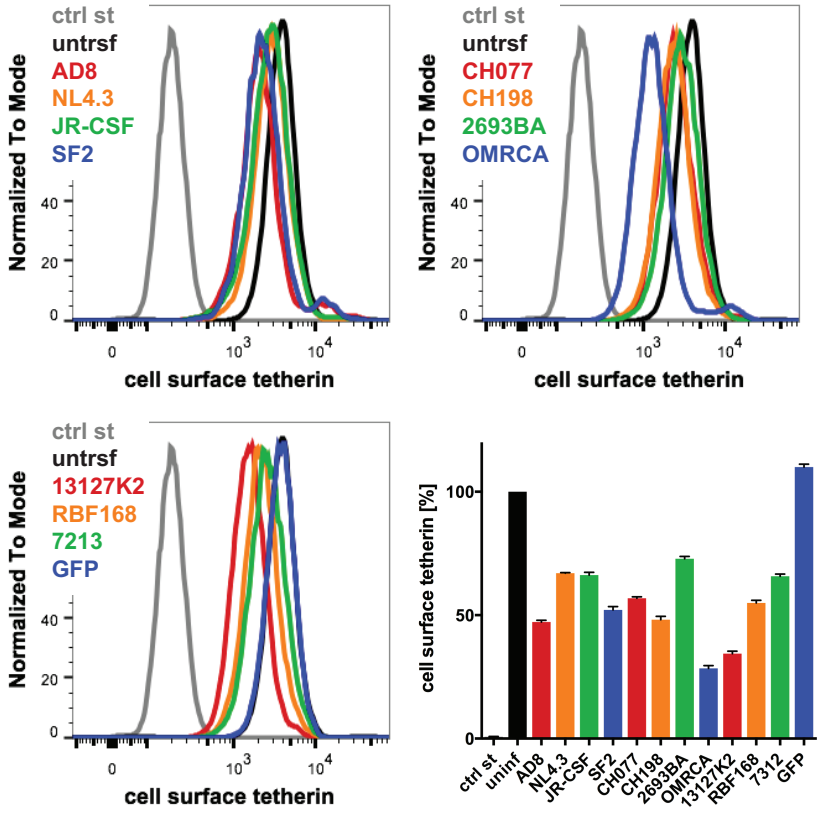

Figure 7: The Nef proteins of different HIV strains show varying degrees of anti-tetherin activity. HeLa cells were transfected with IRES GFP plasmids encoding Nef proteins from a number of HIV strains, and cell surface tetherin levels were quantified by flow cytometry. Mock-transfected cells were immunolabelled with anti-HRP as a staining control. The upper panels and lower left-hand panel show the result from a representative experiment, the lower right-hand panel shows the average relative tetherin levels from four independent experiments ± SEM.

bioRxiv preprint doi: https://doi.org/10.1101/2020.02.07.938464; this version posted February 7, 2020. The copyright holder for this preprint (which was not certified by peer review) is the author/funder, who has granted bioRxiv a license to display the preprint in perpetuity. It is made available under aCC-BY 4.0 International license.

over 50% (Figure 2A). In all our experiments, the anti-tetherin activity of start codon repaired AD8 Vpu was higher than that of Nef. However, we showed that human tetherin downregulation from the cell surface by AD8 Nef is both specific and relevant for reducing AD8 virus retention and promoting AD8 virus release from primary MDM, a natural target of AD8.

We have also shown that AD8 Nef downregulates the cell surface levels of the long isoform of tetherin most likely by increased endocytic sorting of tetherin resulting in its intracellular accumulation (Figure 4, Figure6 and FigureS2). The N-terminal cytoplasmic domain of l-tetherin comprises a serine-threonine-serine (STS) and a conserved dual tyrosine motif. The STS motif can be ubiquitinated [26], whereas the tyrosine motif has been shown to bind the clathrin AP-1 and AP-2 adaptor complexes [27]. Both motifs may cooperate with Vpu to induce tetherin internalisation and/or degradation [26,28]. S-tetherin lacks the twelve N-terminal residues that contain the STS and tyrosine motifs, which may explain why s-tetherin is insensitive to Vpu-mediated removal from the cell surface [21]. By analogy, the lack of AD8 Nef-mediated cell surface downregulation of s-tetherin suggests that AD8 Nef also cooperates with the STS and/or tyrosine motif of l-tetherin to effect cell surface removal of l-tetherin. Cooperation of AD8 Nef with a clathrin adaptor-binding motif in tetherin may explain why mutating AP-2 binding motives in AD8 Nef alone has only a minor effect on its anti-tetherin activity (Figure S2A). Alternatively, the twelve N-terminal residues of l-tetherin may be required for AD8 Nef binding. Interestingly, in contrast to SIVmac Nef proteins that downregulate the cell surface levels of both the l- and s-isoforms of macaque tetherin with equal efficiencies [23], the preference of AD8 Nef for l-tetherin mirrors that of HIV-1 O group Nefs [14].

Our data suggest that AD8 Nef potentiates virus release by lowering the cell surface levels of l-tetherin but does not significantly reduce cell surface or total levels of s-tetherin (Figure 4A, Figure S1A). Nevertheless, AD8 Nef moderately increased virus release from provirus-transfected, s-tetherin-expressing HEK cells in the absence and presence of Vpu (Figure 4B, Figure S1), suggesting that AD8 Nef has some activity against s-tetherin. For efficient viral release it is understood that SIVmac and HIV have alternative mechanisms to counteract s-tetherin [11,23], thus AD8 Nef conferring some activity towards s-tetherin, though unexplained, is reasonable.

Mechanistically, we have shown that a mutant AD8 Nef protein that does not associate with cellular membranes lacks anti-tetherin activity (Figure S2A), and that lower surface tetherin levels are due to increased endocytosis and sequestration of tetherin in perinuclear endosomes (Figure 6). Nef proteins have been shown to modulate cell surface expression of a number of proteins, including MHC-I, CD4, CD8, CD28 and SERINC3/5 [29-31]. The best characterised of these Nef interactions is the one with CD4: HIV Nef proteins are known to bind to cell surface CD4, recruit AP-2 adaptor complexes and thereby promote CD4 internalisation by clathrin-mediated endocytosis. Similarly, we have observed enhanced tetherin internalisation upon transfecting AD8 Nef (Figure 6B); it will be interesting to investigate whether the mechanism of tetherin antagonism by AD8 Nef resembles that of Nef-mediated CD4 downmodulation. Regardless, it is likely that AD8 Nef employs a different mechanism to Vpu to antagonise tetherin as, rather than at the cell surface, Vpu interacts with tetherin in TGN or endosomal compartments and promotes lysosomal sorting of the restriction factor [3,9].

A previous study showed that HIV-1 group O viruses use their Nef proteins to counteract human tetherin [14]. Comparing that study to ours reveals a number of striking similarities: (i) Both group O and AD8 Nef only overcome low levels of tetherin, as found in primary cells; (ii) Both Nef proteins primarily antagonise the long isoform of tetherin; (iii) Group O and AD8 Nef enhance tetherin internalisation that leads, at least in part, to perinuclear accumulation of the restriction factor. However, the group O Nef residues that are key to its anti-tetherin activity are not conserved in AD8 Nef. Instead, we show that both N- and C-terminal domains in AD8 Nef contribute to the reduction in the cell surface levels of human tetherin (Figure 5).

Considering that AD8 Nef is less efficient than Vpu in antagonising tetherin, it is unclear why AD8 would tolerate, or even select for, an easy-to-reverse start codon mutation in Vpu. Accumulating evidence suggests that macrophages are a physiologically relevant reservoir of persistent HIV and SIV infection [32,33]. It has been suggested that inactivation of AD8 Vpu may circumvent an as yet-unknown function detrimental to HIV replication as the virus becomes compartmentalised in macrophages to establish a chronic infection [18]; AD8 Nef may then have adapted to antagonise human tetherin. Alternatively, the redundant anti-tetherin properties of Nef pre-existed the loss of Vpu expression, allowing the loss of Vpu to be tolerated. Importantly, although the anti-tetherin activity of AD8 Nef is weaker than that of Vpu, it appears sufficient to overcome tetherin restriction of virus release in its primary target cells, i.e. macrophages and it is interesting to speculate whether this may have contributed to its tropism.

Whether Nef evolved anti-tetherin function due to the absence of Vpu or this redundant activity was already present and so facilitated the loss of Vpu is unclear. Regardless, whatever the advantage for HIV-1 to use Nef rather than Vpu as a tetherin antagonist, it appears that AD8 may not be the only virus exploiting it. In this study, we found that the Nef proteins from a number of other HIV-1 strains, including two founder

bioRxiv preprint doi: https://doi.org/10.1101/2020.02.07.938464; this version posted February 7, 2020. The copyright holder for this preprint (which was not certified by peer review) is the author/funder, who has granted bioRxiv a license to display the preprint in perpetuity. It is made available under aCC-BY 4.0 International license.

viruses, can reduce cell surface tetherin levels to varying degrees (Figure 7). Moreover, 1.24% of primary isolates in the HIV database encode a Vpu start codon mutation [34], and it will be intriguing to investigate whether some of these viruses use their Nef proteins to overcome tetherin restriction.

Funding Information

This work was supported by UK Medical Research Council funding to the MRC-UCL LMCB University Unit (MC_UU00012/1 and MC_U12266B) and an MRC Centenary Award to SG. The funders had no role in study design, data collection and interpretation, or the decision to submit the work for publication.

Acknowledgements

We thank K. Strebel, S. Neil, M. Harris, G. Towers, C. Jolly, the NIH AIDS Reagent Program, and the NIBSC Centre for AIDS Reagents for plasmids, cell lines and antibodies. We are grateful to S. Czieso for technical assistance.

Author contributions

Conceptualization, S.G. and Ma.M.; Methodology, S.G., S.L. and Mi.M.; Formal Analysis, S.G., S.L. and Mi.M.; Investigation, S.G., S.L., Mi.M. and B.M.N.; Writing – Original Draft Preparation, S.G., S.L. and Mi.M.; Visualisation, S.G., S.L. and Mi.M. Writing – Review & Editing, S.G., S.L., Mi.M. and Ma.M. Funding Acquisition, S.G. and Ma.M.

References

1. Gupta, R.K.; Towers, G.J. A tail of Tetherin: how pandemic HIV-1 conquered the world. *Cell Host Microbe* **2009**, *6*, 393-395, doi:10.1016/j.chom.2009.11.002.

2. Sauter, D.; Schindler, M.; Specht, A.; Landford, W.N.; Munch, J.; Kim, K.A.; Votteler, J.; Schubert, U.; Bibollet-Ruche, F.; Keele, B.F., et al. Tetherin-driven adaptation of Vpu and Nef function and the evolution of pandemic and nonpandemic HIV-1 strains. *Cell Host Microbe* **2009**, *6*, 409-421, doi:10.1016/j.chom.2009.10.004.

3. Neil, S.J. The antiviral activities of tetherin. *Curr Top Microbiol Immunol* **2013**, *371*, 67-104, doi:10.1007/978-3-642-37765-5_3.

4. Venkatesh, S.; Bieniasz, P.D. Mechanism of HIV-1 virion entrapment by tetherin. *PLoS Pathog* **2013**, *9*, e1003483, doi:10.1371/journal.ppat.1003483.

5. Neil, S.J.; Zang, T.; Bieniasz, P.D. Tetherin inhibits retrovirus release and is antagonized by HIV-1 Vpu. *Nature* **2008**, *451*, 425-430, doi:10.1038/nature06553.

6. Van Damme, N.; Goff, D.; Katsura, C.; Jorgenson, R.L.; Mitchell, R.; Johnson, M.C.; Stephens, E.B.; Guatelli, J. The interferon-induced protein BST-2 restricts HIV-1 release and is downregulated from the cell surface by the viral Vpu protein. *Cell Host Microbe* **2008**, *3*, 245-252, doi:10.1016/j.chom.2008.03.001.

7. Giese, S.M., M. *Cellular Trafficking Mechanisms in the Assembly and Release of HIV.*; Springer New York: 2013.

8. Douglas, J.L.; Viswanathan, K.; McCarroll, M.N.; Gustin, J.K.; Fruh, K.; Moses, A.V. Vpu directs the degradation of the human immunodeficiency virus restriction factor BST-2/Tetherin via a {beta}TrCP-dependent mechanism. *J Virol* **2009**, *83*, 7931-7947, doi:10.1128/JVI.00242-09.

9. Janvier, K.; Pelchen-Matthews, A.; Renaud, J.B.; Caillet, M.; Marsh, M.; Berlioz-Torrent, C. The ESCRT-0 component HRS is required for HIV-1 Vpu-mediated BST-2/tetherin down-regulation. *PLoS Pathog* **2011**, *7*, e1001265, doi:10.1371/journal.ppat.1001265.

10. Mangeat, B.; Gers-Huber, G.; Lehmann, M.; Zufferey, M.; Luban, J.; Piguet, V. HIV-1 Vpu neutralizes the antiviral factor Tetherin/BST-2 by binding it and directing its beta-TrCP2-dependent degradation. *PLoS Pathog* **2009**, *5*, e1000574, doi:10.1371/journal.ppat.1000574.

11. McNatt, M.W.; Zang, T.; Bieniasz, P.D. Vpu binds directly to tetherin and displaces it from nascent virions. *PLoS Pathog* **2013**, *9*, e1003299, doi:10.1371/journal.ppat.1003299.

12. Mitchell, R.S.; Katsura, C.; Skasko, M.A.; Fitzpatrick, K.; Lau, D.; Ruiz, A.; Stephens, E.B.; Margottin-Goguet, F.; Benarous, R.; Guatelli, J.C. Vpu antagonizes BST-2-mediated restriction of HIV-1 release via beta-TrCP and endo-lysosomal trafficking. *PLoS Pathog* **2009**, *5*, e1000450, doi:10.1371/journal.ppat.1000450.

13. Le Tortorec, A.; Neil, S.J. Antagonism to and intracellular sequestration of human tetherin by the human immunodeficiency virus type 2 envelope glycoprotein. *J Virol* **2009**, *83*, 11966-11978, doi:10.1128/JVI.01515-09.

14. Kluge, S.F.; Mack, K.; Iyer, S.S.; Pujol, F.M.; Heigele, A.; Learn, G.H.; Usmani, S.M.; Sauter, D.; Joas, S.; Hotter, D., et al. Nef proteins of epidemic HIV-1 group O strains antagonize human tetherin. *Cell Host Microbe* **2014**, *16*, 639-650, doi:10.1016/j.chom.2014.10.002.

bioRxiv preprint doi: https://doi.org/10.1101/2020.02.07.938464; this version posted February 7, 2020. The copyright holder for this preprint (which was not certified by peer review) is the author/funder, who has granted bioRxiv a license to display the preprint in perpetuity. It is made available under aCC-BY 4.0 International license.

15. Zhang, F.; Wilson, S.J.; Landford, W.C.; Virgen, B.; Gregory, D.; Johnson, M.C.; Munch, J.; Kirchhoff, F.; Bieniasz, P.D.; Hatziioannou, T. Nef proteins from simian immunodeficiency viruses are tetherin antagonists. *Cell Host Microbe* **2009**, *6*, 54-67, doi:10.1016/j.chom.2009.05.008.

16. Zhang, F.; Landford, W.N.; Ng, M.; McNatt, M.W.; Bieniasz, P.D.; Hatziioannou, T. SIV Nef proteins recruit the AP-2 complex to antagonize Tetherin and facilitate virion release. *PLoS Pathog* **2011**, *7*, e1002039, doi:10.1371/journal.ppat.1002039.

17. Jia, B.; Serra-Moreno, R.; Neidermyer, W.; Rahmberg, A.; Mackey, J.; Fofana, I.B.; Johnson, W.E.; Westmoreland, S.; Evans, D.T. Species-specific activity of SIV Nef and HIV-1 Vpu in overcoming restriction by tetherin/BST2. *PLoS Pathog* **2009**, *5*, e1000429, doi:10.1371/journal.ppat.1000429.

18. Schubert, U.; Bour, S.; Willey, R.L.; Strebel, K. Regulation of virus release by the macrophage-tropic human immunodeficiency virus type 1 AD8 isolate is redundant and can be controlled by either Vpu or Env. *J Virol* **1999**, *73*, 887-896.

19. Theodore, T.S.; Englund, G.; Buckler-White, A.; Buckler, C.E.; Martin, M.A.; Peden, K.W. Construction and characterization of a stable full-length macrophage-tropic HIV type 1 molecular clone that directs the production of high titers of progeny virions. *AIDS Res Hum Retroviruses* **1996**, *12*, 191-194, doi:10.1089/aid.1996.12.191.

20. Schubert, U.; Clouse, K.A.; Strebel, K. Augmentation of virus secretion by the human immunodeficiency virus type 1 Vpu protein is cell type independent and occurs in cultured human primary macrophages and lymphocytes. *J Virol* **1995**, *69*, 7699-7711.

21. Cocka, L.J.; Bates, P. Identification of alternatively translated Tetherin isoforms with differing antiviral and signaling activities. *PLoS Pathog* **2012**, *8*, e1002931, doi:10.1371/journal.ppat.1002931.

22. Galao, R.P.; Le Tortorec, A.; Pickering, S.; Kueck, T.; Neil, S.J. Innate sensing of HIV-1 assembly by Tetherin induces NFkappaB-dependent proinflammatory responses. *Cell Host Microbe* **2012**, *12*, 633-644, doi:10.1016/j.chom.2012.10.007.

23. Weinelt, J.; Neil, S.J. Differential sensitivities of tetherin isoforms to counteraction by primate lentiviruses. *J Virol* **2014**, *88*, 5845-5858, doi:10.1128/JVI.03818-13.

24. Yu, G.; Felsted, R.L. Effect of myristoylation on p27 nef subcellular distribution and suppression of HIV-LTR transcription. *Virology* **1992**, *187*, 46-55, doi:10.1016/0042-6822(92)90293-x.

25. Richards, K.H.; Clapham, P.R. Effects of vpu start-codon mutations on human immunodeficiency virus type 1 replication in macrophages. *J Gen Virol* **2007**, *88*, 2780-2792, doi:10.1099/vir.0.83120-0.

26. Tokarev, A.A.; Munguia, J.; Guatelli, J.C. Serine-threonine ubiquitination mediates downregulation of BST-2/tetherin and relief of restricted virion release by HIV-1 Vpu. *J Virol* **2011**, *85*, 51-63, doi:10.1128/JVI.01795-10.

27. Rollason, R.; Korolchuk, V.; Hamilton, C.; Schu, P.; Banting, G. Clathrin-mediated endocytosis of a lipid-raft-associated protein is mediated through a dual tyrosine motif. *J Cell Sci* **2007**, *120*, 3850-3858, doi:10.1242/jcs.003343.

28. Kueck, T.; Neil, S.J. A cytoplasmic tail determinant in HIV-1 Vpu mediates targeting of tetherin for endosomal degradation and counteracts interferon-induced restriction. *PLoS Pathog* **2012**, *8*, e1002609, doi:10.1371/journal.ppat.1002609.

29. Landi, A.; Iannucci, V.; Nuffel, A.V.; Meuwissen, P.; Verhasselt, B. One protein to rule them all: modulation of cell surface receptors and molecules by HIV Nef. *Curr HIV Res* **2011**, *9*, 496-504, doi:10.2174/157016211798842116.

30. Matheson, N.J.; Sumner, J.; Wals, K.; Rapiteanu, R.; Weekes, M.P.; Vigan, R.; Weinelt, J.; Schindler, M.; Antrobus, R.; Costa, A.S., et al. Cell Surface Proteomic Map of HIV Infection Reveals Antagonism of Amino Acid Metabolism by Vpu and Nef. *Cell Host Microbe* **2015**, *18*, 409-423, doi:10.1016/j.chom.2015.09.003.

31. Usami, Y.; Wu, Y.; Gottlinger, H.G. SERINC3 and SERINC5 restrict HIV-1 infectivity and are counteracted by Nef. *Nature* **2015**, *526*, 218-223, doi:10.1038/nature15400.

32. Clayton, K.L.; Garcia, J.V.; Clements, J.E.; Walker, B.D. HIV Infection of Macrophages: Implications for Pathogenesis and Cure. *Pathog Immun* **2017**, *2*, 179-192, doi:10.20411/pai.v2i2.204.

33. Wong, M.E.; Jaworowski, A.; Hearps, A.C. The HIV Reservoir in Monocytes and Macrophages. *Front Immunol* **2019**, *10*, 1435, doi:10.3389/fimmu.2019.01435.

bioRxiv preprint doi: https://doi.org/10.1101/2020.02.07.938464; this version posted February 7, 2020. The copyright holder for this preprint (which was not certified by peer review) is the author/funder, who has granted bioRxiv a license to display the preprint in perpetuity. It is made available under aCC-BY 4.0 International license.

34. Dejucq, N.; Simmons, G.; Clapham, P.R. T-cell line adaptation of human immunodeficiency virus type 1 strain SF162: effects on envelope, vpu and macrophage-tropism. *J Gen Virol* **2000**, *81*, 2899-2904, doi:10.1099/0022-1317-81-12-2899.

35. Giese, S.; Marsh, M. Tetherin can restrict cell-free and cell-cell transmission of HIV from primary macrophages to T cells. *PLoS Pathog* **2014**, *10*, e1004189, doi:10.1371/journal.ppat.1004189.

36. Pelchen-Matthews, A.; Kramer, B.; Marsh, M. Infectious HIV-1 assembles in late endosomes in primary macrophages. *J Cell Biol* **2003**, *162*, 443-455, doi:10.1083/jcb.200304008.

37. Chaudhuri, R.; Lindwasser, O.W.; Smith, W.J.; Hurley, J.H.; Bonifacino, J.S. Downregulation of CD4 by human immunodeficiency virus type 1 Nef is dependent on clathrin and involves direct interaction of Nef with the AP2 clathrin adaptor. *J Virol* **2007**, *81*, 3877-3890, doi:10.1128/JVI.02725-06.

38. Lindwasser, O.W.; Smith, W.J.; Chaudhuri, R.; Yang, P.; Hurley, J.H.; Bonifacino, J.S. A diacidic motif in human immunodeficiency virus type 1 Nef is a novel determinant of binding to AP-2. *J Virol* **2008**, *82*, 1166-1174, doi:10.1128/JVI.01874-07.

Supplementary Material

Name	Vector	Origin	Description
AD8(+)	pBR322	K. Strebel (NIAID, Bethesda, USA)	See reference (19).
AD8(-)	pBR322	K. Strebel (NIAID, Bethesda, USA)	See reference (19).
AD8(U_{del2})	pBR322	K. Strebel (NIAID, Bethesda, USA)	See reference (20).
AD8(+)ΔNef	pBR322	this study	Nef-deficient AD8(+). Nef frame shift mutation introduced using the primers 5'-GGCCT ACTGT AAGGG AAAGA ATAGA CACGA GCTGA GC-3' and 5'-GCTCA GCTCG TGTCT ATTCT TTCCC TTACA GTAGG CC-3', and the QuikChange II XL Site-Directed Mutagenesis Kit (Agilent Technologies, Wokingham, UK) according to the manufacturer's instructions.
AD8(-)ΔNef	pBR322	this study	Nef-deficient AD8(-). Nef frame shift mutation introduced as described for AD8(+)ΔNef.
AD8(U_{del2})ΔNef	pBR322	this study	Nef-deficient AD8(U_{del2}). Nef frame shift mutation introduced as described for AD8(+)ΔNef.
VSVG	pMDG	G. Towers (UCL, London, UK)	-
AD8 Nef wild type	pcDNA3.1(+)	this study	The Nef open reading frame (ORF) was amplified from AD8(+) and inserted into pcDNA3.1 using BamH1 and EcoR1 restriction sites.
AD8 Vpu	pcDNA3.1(+)	this study	The Vpu open reading frame (ORF) was amplified from AD8(+) and inserted into pcDNA3.1 using BamH1 and EcoR1 restriction sites.
AD8 Env	pcDNA3.1(+)	this study	The Env open reading frame (ORF) was amplified from AD8(-) and inserted into pcDNA3.1 using BamH1 and EcoR1 restriction sites.
HIV-1 Rev	pBC12/CMV	G. Towers (UCL, London, UK)	-
AD8 Nef E160A_LL164/165AA	pcDNA3.1(+)	this study	The mutations LL164/165AA and E160A were consecutively introduced into AD8 Nef wild type using the primers 5'-CAATA AAGGA GAGAA CAACT GCGCG GCACA CCCTA TGAGC CAGCA TGGA-3' and 5'-TCCAT GCTGG CTCAT AGGGT GTGCC GCGCA GTTGT TCTCT CCTTT ATTG-3', and 5'-AGGCC AATAA AGGAG CGAAC AACTG CGCGG C-3' and 5'-GCCGC GCAGT TGTTC GCTCC TTTAT TGGCC T-3', respectively, and the QuikChange II Site-Directed Mutagenesis Kit (Agilent Technologies) according to the manufacturer's instructions.
AD8 Nef DD174/175RA	pcDNA3.1(+)	this study	The mutation was introduced into AD8 Nef wild type using the primers 5'-CAACA CTTCT CTCTC CGTGG CACGC ATTCC ATGCT GGCTC ATA-3' and 5'-TATGA GCCAG CATGG AATGC GTGCC ACGGA GAGAG AAGTG TTG-3', and the QuikChange II Site-Directed Mutagenesis Kit (Agilent Technologies) according to the manufacturer's instructions.

bioRxiv preprint doi: https://doi.org/10.1101/2020.02.07.938464; this version posted February 7, 2020. The copyright holder for this preprint (which was not certified by peer review) is the author/funder, who has granted bioRxiv a license to display the preprint in perpetuity. It is made available under aCC-BY 4.0 International license.

AD8 Nef E160A_LL164/165AA_ DD174/175RA	pcDNA3.1(+)	this study	The mutation DD174/175RA was introduced into AD8 Nef E160A_LL164/165A using the primers listed above and the QuikChange II Site-Directed Mutagenesis Kit (Agilent Technologies) according to the manufacturer's instructions.
AD8 Nef G2A	pcDNA3.1(+)	this study	The mutation was introduced into AD8 Nef wild type using the primers 5'-CTCGG ATCCA AGATG GCTGG CAAGT GGTCA AAA-3' and 5'-TTTTG ACCAC TTGCC AGCCA TCTTG GATCC GAG-3', and the QuikChange II Site-Directed Mutagenesis Kit (Agilent Technologies) according to the manufacturer's instructions.
NL4.3 Nef	pcDNA3.1(+)	this study	The Nef open reading frame (ORF) was amplified from pNL4.3 (provided by C. Jolly, UCL, London, UK) and inserted into pcDNA3.1 using BamH1 and EcoR1 restriction sites.
AD8-NL4.3 Nef	pcDNA3.1(+)	this study	The N-terminal AD8 Nef domain was excised from AD8 Nef wild type using BamH1 and Bgl2 and ligated into NL4.3 Nef digested with the same restriction enzymes.
NL4.3-AD8 Nef	pcDNA3.1(+)	this study	The N-terminal NL4.3 Nef domain was excised from NL4.3 Nef using BamH1 and Bgl2 and ligated into AD8 Nef wild type digested with the same restriction enzymes.
AD8 Nef IRES GFP	pCG	this study	The ORF was inserted into pCG using Xba1 and Mlu1 restriction sites.
NL4.3 Nef IRES GFP	pCG	modified in this study (originally obtained from F. Kirchhoff, University of Ulm, Germany)	The ORF was inserted into pCG using Xba1 and Mlu1 restriction sites.
JR-CSF Nef IRES GFP	pCG	F. Kirchhoff (University of Ulm, Germany)	-
SF2 Nef IRES GFP	pCG	F. Kirchhoff (University of Ulm, Germany)	-
CH077 Nef IRES GFP	pCG	F. Kirchhoff (University of Ulm, Germany)	-
CH198 Nef IRES GFP	pCG	F. Kirchhoff (University of Ulm, Germany)	-
2693BA Nef IRES GFP	pCG	F. Kirchhoff (University of Ulm, Germany)	-
OMRCA Nef IRES GFP	pCG	modified in this study (originally obtained from F. Kirchhoff, University of Ulm, Germany)	The ORF was inserted into pCG using Xba1 and Mlu1 restriction sites.
13127K2 Nef IRES GFP	pCG	F. Kirchhoff (University of Ulm, Germany)	-
RBF168 Nef IRES GFP	pCG	F. Kirchhoff (University of Ulm, Germany)	-
7312 Nef IRES GFP	pCG	modified in this study (originally obtained from F. Kirchhoff, University of Ulm, Germany)	The ORF was inserted into pCG using Xba1 and Mlu1 restriction sites.
NL4.3 Nef_stop IRES GFP	pCG	F. Kirchhoff (University of Ulm, Germany)	-

Table S1: Origins and descriptions of DNA plasmids used in this study.

bioRxiv preprint doi: https://doi.org/10.1101/2020.02.07.938464; this version posted February 7, 2020. The copyright holder for this preprint (which was not certified by peer review) is the author/funder, who has granted bioRxiv a license to display the preprint in perpetuity. It is made available under aCC-BY 4.0 International license.

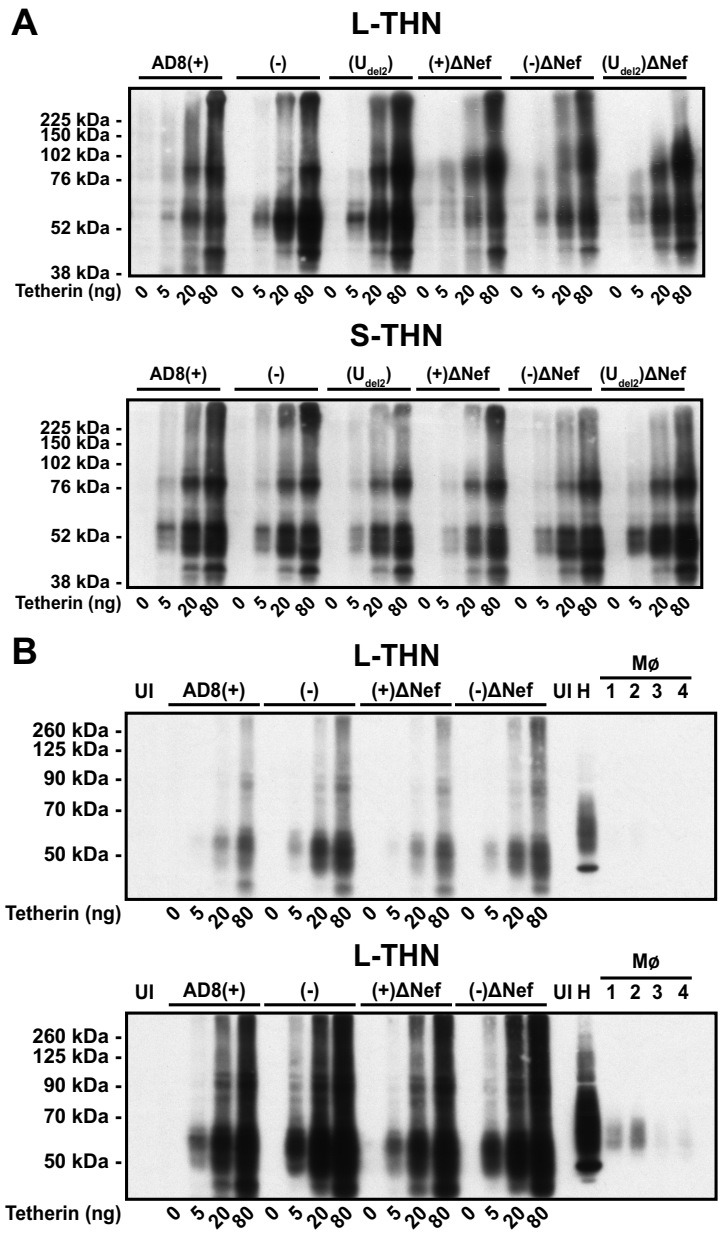

Figure S1: AD8 Nef enhances virus release at low tetherin concentrations. (A) Analysis of tetherin expression levels in the HEK 293T cells used for Figure 4B. HEK 293T cells were transfected with 400 ng of HIV-1 AD8 proviral DNA and increasing amounts of l- or s-tetherin-encoding plasmids. Cells were harvested two days post transfection and all lysates were analysed by western blotting. (B) HeLa cells express high levels, and MDMs low levels of endogenous tetherin. Tetherin expression levels of the HEK 293T cells used for Figure 4B were compared to endogenous tetherin levels in HeLa cells and MDMs. HEK 293T samples were prepared as described for (A) and analysed by western blotting alongside cell lysates from HeLa and MDMs (four different donors denoted 1-4). All samples were derived from equal numbers of cells. The upper and lower panels show the same blot at a low and a high exposure, respectively.

bioRxiv preprint doi: https://doi.org/10.1101/2020.02.07.938464; this version posted February 7, 2020. The copyright holder for this preprint (which was not certified by peer review) is the author/funder, who has granted bioRxiv a license to display the preprint in perpetuity. It is made available under aCC-BY 4.0 International license.

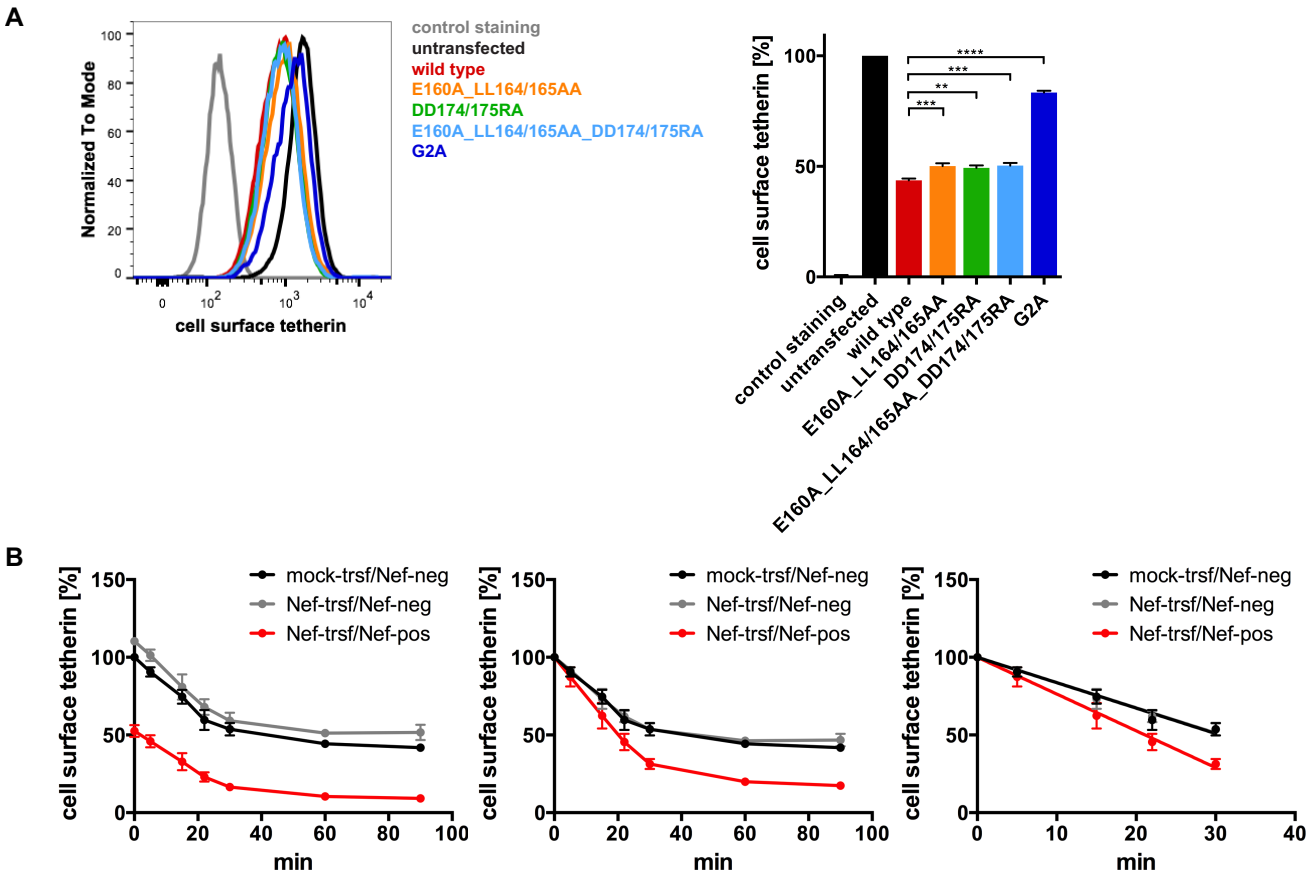

Figure S2: HIV-1 AD8 Nef enhances tetherin internalisation. (A) HeLa cells were transfected with AD8 Nef wild type or indicated mutants, and cell surface tetherin levels were quantified by flow cytometry. Mock-transfected cells were immunolabelled with anti-HRP as a staining control. The E160A_LL164/165AA and DD174/175RA mutations disrupt Nef interactions with AP-2 adaptor complexes [37,38], the G2A mutation disrupts a myristoylation signal. The left-hand panel shows the result from a representative experiment, the right-hand panel the average relative tetherin levels from six independent experiments ± SEM. Statistical significance was calculated using the ANOVA test. (B) Analysis of the tetherin internalisation experiment shown in Figure 6B. AD8 Nef- or mock-transfected HeLa cells were immunolabelled for tetherin on ice and shifted to 37°C for various times. Residual cell surface tetherin antibody was then revealed by immunostaining on ice using a fluorescent secondary antibody. Cells were fixed, permeabilised, immunostained for Nef and analysed by flow cytometry. The left-hand, central and right-hand panels show the average relative tetherin levels of four independent experiments ± SEM before normalisation, after normalisation, and after linear regression analysis of the first 30 min at 37°C, respectively.

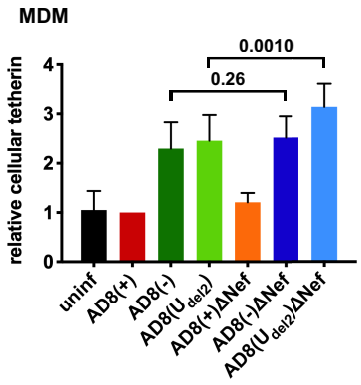

Figure S3: Quantification of cellular tetherin levels in HIV-1 AD8-infected MDMs. HIV-1 AD8-infected MDMs were harvested and the lysates were analysed by western blotting as described in Figure 3B. The graphs show the average relative tetherin levels from four donors ± SEM with relevant P values.